Epidemic threshold and topological structure of susceptible-infectious-susceptible epidemics in adaptive networks

Dongchao Guo,[1,2,*] Stojan Trajanovski,[1,†] Ruud van de Bovenkamp,[1] Huijuan Wang,[1] and Piet Van Mieghem[1]

[1]*Faculty of Electrical Engineering, Mathematics and Computer Science, Delft University of Technology, P.O. Box 5031, 2600 GA Delft, The Netherlands*

[2]*Institute of Information Science, Beijing Jiaotong University, 100044 Beijing, People's Republic of China*

The interplay between disease dynamics on a network and the dynamics of the structure of that network characterizes many real-world systems of contacts. A continuous-time adaptive susceptible-infectious-susceptible (ASIS) model is introduced in order to investigate this interaction, where a susceptible node avoids infections by breaking its links to its infected neighbors while it enhances the connections with other susceptible nodes by creating links to them. When the initial topology of the network is a complete graph, an exact solution to the average metastable-state fraction of infected nodes is derived without resorting to any mean-field approximation. A linear scaling law of the epidemic threshold τ_c as a function of the effective link-breaking rate ω is found. Furthermore, the bifurcation nature of the metastable fraction of infected nodes of the ASIS model is explained. The metastable-state topology shows high connectivity and low modularity in two regions of the τ,ω plane for any effective infection rate $\tau > \tau_c$: (i) a "strongly adaptive" region with very high ω and (ii) a "weakly adaptive" region with very low ω. These two regions are separated from the other half-open elliptical-like regions of low connectivity and high modularity in a contour-line-like way. Our results indicate that the adaptation of the topology in response to disease dynamics suppresses the infection, while it promotes the network evolution towards a topology that exhibits assortative mixing, modularity, and a binomial-like degree distribution.

I. INTRODUCTION

Recently, the coupling between epidemic dynamics and the underlying network topology has attracted ample attention [1–3]. A network, where the topology changes independently from the epidemic spread, is called an evolving network. In an evolving network, where the topology changes based on some predefined patterns, the epidemic threshold has been investigated in a number of studies [4,5]. More complex than evolving networks are adaptive networks, where the topology changes in response to the epidemic process. In other words, there exists an interplay between the dynamics *of* the network (i.e., the change of the topology) and the dynamics *on* the network (i.e., the epidemic process).

Gross *et al.* [6] proposed an adaptive network model, where a rewiring process is introduced in the classical susceptible-infected-susceptible (SIS) model. In every time step, for every link connecting a susceptible node with an infected node (i.e., S-I link), the susceptible node is infected with probability *p*. The infected node recovers with probability *r*. Meanwhile, for every S-I link, the susceptible node breaks the S-I link with probability *w* and immediately reconnects the link to another randomly selected susceptible node. The link-breaking and reconnecting process is an instance of a *rewiring process*. Gross *et al.* [6] reported a complex bifurcation pattern during the evolution of the adaptive network through the healthy state, the oscillatory state, the bistable state and the endemic state, respectively, as *p* increases with fixed nonzero *r* and *w*. An improved analysis of Gross's model was presented by Marceau

et al. [7], while the model of Zanette and Risau-Gusmán [8] differs from that of Gross *et al.* [6] in that the broken link is reconnected to a randomly selected, but not necessarily susceptible node. Lagorio *et al.* [9] studied the discrete-time susceptible-infected-recovered (SIR) model in the presence of a rewiring process and argued that there exists a phase transition at a critical rewiring rate w_c.

Valdez *et al.* [10] proposed an adaptive SIR model, where a link-activation-deactivation strategy different from the *link rewiring* is introduced to the classical SIR model. In every discrete time step and for every S-I link, the infected node *i* infects its susceptible neighbor *j* with probability *p*. Otherwise, if the node *i* fails to infect its neighbor *j*, with probability σ, its neighbor *j* breaks (deactivates) the link connected to node *i* for a fixed period t_B. After t_B time steps, the link between nodes *i* and *j* will be created (activated) again. Every infected node *i* recovers after a fixed period t_R. In contrast to the *link-rewiring* process in Gross's adaptive model [6] which is a global link-dynamic process, following the link-dynamic strategy proposed in [10], a link can only be broken (deactivated) and created (activated) based on the local information (i.e., the viral states of nodes connected by the link). There exists a threshold σ_c above which the epidemic dies out according to Valdez *et al.* [10]. A SIS model with link-activation-deactivation dynamics was investigated by Tunc *et al.* [11].

The above related papers on adaptive networks mainly concentrate on the persistence of the epidemic on the network by studying the epidemic threshold of the adaptive network in the metastable state. However, all these papers are based on mean-field approximations ignoring high-order correlations. On the other hand, the formation of special structures when the adaptive network is in the metastable state, such as the

*08112070@bjtu.edu.cn

†s.trajanovski@tudelft.nl

emergence of a highly connected susceptible component as well as the associated degree distribution [6], have rarely been discussed in detail. Wieland *et al.* [12] addressed how the degree distribution converges to a well-defined distribution irrespective of the initial topology in the adaptive SIS model of Gross *et al.* [6]. Using stochastic differential equations, Rogers *et al.* [13] investigated the mean degree of susceptible nodes in adaptive networks.

In this paper, we propose a continuous-time adaptive SIS model (in short, *ASIS model*) where a new link-dynamic strategy is introduced into the SIS model. The paper is organized as follows. Section II describes the ASIS model and its generality compared with other adaptive SIS models. Section III explains the simulation method that we employ to calculate the metastable-state characteristics of the ASIS model. Section IV constitutes the main part of this article. When the initial topology is a complete graph, we first propose and verify an exact formula for the average metastable-state fraction *y* of infected nodes. Next, we discuss and calculate the epidemic threshold of the ASIS model. Then we show the impact of the disease dynamics and the link dynamics on the metastable-state topology by investigating many characteristics of the metastable topology such as the modularity [14], the connectivity [15], and the degree distribution. We show a complex bifurcation diagram of the metastable fraction of infected nodes observed from the ASIS model. Finally, we conclude the paper in Sec. V.

II. ADAPTIVE SIS MODEL

A. Model description

We consider the interplay between the virus spread and the topology change in an undirected graph $G(N,L)$ with N nodes and L links denoted by a symmetric adjacency matrix A. The viral state of node i at time t is specified by a Bernoulli random variable $X_i(t) \in \{0,1\}$: $X_i(t) = 1$ for an infected node and $X_i(t) = 0$ for a susceptible node. At time t, a node i can be in one of the two possible states: *infected*, with probability $v_i(t) = \Pr[X_i(t) = 1]$ or *healthy*, with probability $1 - v_i(t)$, but susceptible to the virus. We assume that the curing process per infected node is a Poisson process with rate δ, and that the infection process per link connecting an infected node and a susceptible node is a Poisson process with rate β. Both the curing and the infection Poisson processes are independent. Only when a node i is infected can it infect its direct neighbors that are still susceptible. This is the general description of the simplest type of the continuous-time susceptible-infected-susceptible (SIS) epidemic model.

We now describe the link-dynamic process, reflected by an adjacency matrix $A(t)$ at time t. Each element $a_{ij}(t)$ of $A(t)$ is a Bernoulli random variable $a_{ij}(t) \in \{0,1\}$, which specifies the existence of the link between nodes i and j: When $a_{ij}(t) = 1$, there is a link between nodes i and j at time t with probability $\Pr[a_{ij}(t) = 1]$, and, when $a_{ij}(t) = 0$, there is no link with probability $1 - \Pr[a_{ij}(t) = 1]$. Two processes, the link-breaking [Fig. 1(a)] and the link-creating [Fig. 1(b)], run independently based on the viral state of the end nodes of the link. Suppose that node i and node j were initially connected, i.e., $a_{ij}(0) = 1$. Once one of them, but not both, is infected,
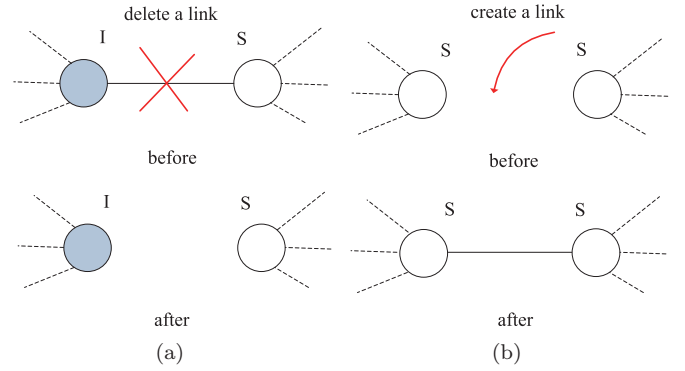

FIG. 1. (Color online) Link state changing based on the viral states of a pair of nodes. (a) The link breaking between the susceptible node (S) and the infected node (I); (b) the link creating between a pair of susceptible nodes (S).

the link (i,j) between them can be broken (deactivated). The link-breaking process is a Poisson process with rate ζ. Given that the link between nodes i and j was broken (deactivated) at one time, a link can be recreated (activated) between them once both node i and node j are susceptible. The link-creating process is a Poisson process with rate ξ.

B. Model formulation

Taking the Bernoullian nature, $E[X_i] = \Pr[X_i = 1]$, into account, we formulate the change of the viral state of node i as

$$\frac{d}{dt} E[X_i] = E\left[-\delta X_i + (1 - X_i)\beta \sum_{j=1}^{N} a_{ij} X_j\right], \quad (1)$$

where the right-hand side of (1) is composed of two parts: While being infected, node i is cured with rate δ, and while node i is healthy, it can be infected by each of its infected neighbors with rate β. In the same manner, using the Bernoullian property $E[X^n] = E[X]$ for any integer $n > 1$, we define the change of the link $a_{ij}(t)$ as

$$\begin{aligned}
\frac{d}{dt} E[a_{ij}] &= a_{ij}(0) E\{-\zeta a_{ij}[X_i(1 - X_j) + X_j(1 - X_i)] \\
&\quad + \xi(1 - a_{ij})(1 - X_i)(1 - X_j)\} \\
&= a_{ij}(0) E[-\zeta a_{ij}(X_i - X_j)^2 \\
&\quad + \xi(1 - a_{ij})(1 - X_i)(1 - X_j)], \quad (2)
\end{aligned}$$

where the right-hand side of (2) consists of two opposing processes. (i) While either node i or node j, but not both, is infected, the link between nodes i and j is broken (deactivated, removed) with rate ζ in order to protect the susceptible node from infection as shown in Fig. 1(a). (ii) While both node i and node j are susceptible, a link is created between them with rate ξ as shown in Fig. 1(b) given that the link (i,j) existed in the original topology [i.e., $a_{ij}(0) = 1$]. In the case when both node i and node j are infected (i.e., $X_i = X_j = 1$), the link is preserved, i.e., $\frac{dE[a_{ij}]}{dt} = 0$. In the following, the above model, consisting of governing equations (1) and (2), is named the *adaptive SIS model*, or *ASIS model* in short. Before proceeding, we recast the governing equations (1) and (2) in a

dimensionless form by defining

$$\tilde{t} = t\delta, \quad \tilde{\zeta} = \frac{\zeta}{\delta}, \quad \tilde{\xi} = \frac{\xi}{\delta}, \quad \tau = \frac{\beta}{\delta}, \quad \omega = \frac{2\zeta}{\xi}, \quad (3)$$

where τ is the effective infection rate, ω is the effective link-breaking rate, and the time $\tilde{t}$ is measured in units of the curing rate δ. In the following, we drop the tilde ($\tilde{\ }$) notation and work with the dimensionless parameters (3). Employing the dimensionless variables (3), the dimensionless forms of (1) and (2) are

$$\frac{d}{dt}E[X_i] = E\left[-X_i + (1 - X_i)\tau \sum_{j=1}^{N} a_{ij}X_j\right], \quad (4)$$

$$\frac{d}{dt}E[a_{ij}] = a_{ij}(0)E[-\zeta a_{ij}(X_i - X_j)^2 + \xi(1 - a_{ij})(1 - X_i)(1 - X_j)]. \quad (5)$$

In this paper, we confine ourselves to the complete graph K_N, where $a_{ij}(0) = 1$ for any nodal pair (i, j). Only for K_N, an exact analysis (see Theorem 1 below) is possible.

As explained in Sec. III, the steady state of the ASIS model in a finite-size network is the purely healthy state. Therefore, the metastable state of the ASIS model is of interest, in which the system (consisting of the disease dynamics and link dynamics) remains for a long time before being trapped into the absorbing steady state.

C. Generality of the ASIS model

By slightly recasting the governing equations (1) and (2), our proposed ASIS model can be reduced to some other models. When a new link can be created between any pair of healthy nodes, Gross *et al.*'s model [6] elaborated in Sec. I applies. Denote by p, r, and w the infection probability, the curing probability, and the rewiring probability, respectively, in Gross's model. The rewiring process in Gross's model actually consists of two subprocesses: Within a time step, a susceptible node i (a) first breaks the link connected to its infected neighbor j with probability w and (b) then immediately creates a link to another randomly selected susceptible node. The link-breaking subprocess depends on the viral states of both nodes and happens with probability w. Once the link-breaking subprocess occurs, the link-creating subprocess follows that increases the degree of another susceptible node disconnected from i by 1 with probability $1/N_i$, where N_i is the number of these susceptible nodes. By employing the term $a_{ij}(0) = 1$ for any nodal pair (i, j) and

$$\beta = p, \delta = r, \zeta = w, \xi_{ij} = \frac{R_i}{N_i} + \frac{R_j}{N_j} - \frac{R_i R_j}{N_i N_j},$$

$$R_i = \zeta \sum_{m=1}^{N} a_{im}(t)[1 - X_i(t)]X_m(t), \quad (6)$$

$$N_i = \sum_{m=1}^{N}[1 - a_{im}(t)][1 - X_i(t)][1 - X_m(t)],$$

in the governing equation (2), our proposed ASIS model reduces to one similar to Gross's model [6], although there is only one link-dynamic process (i.e., the rewiring process) in Gross' model [6], while two separate link dynamics (i.e., the

link-breaking process and the link-creating process) exist in the ASIS model. The term ξ_{ij} denotes the link-creating rate which depends on node i and j. The term R_i denotes the average number of links connected to node i which are broken within a time step, while N_i equals the number of the susceptible nodes disconnected from i. The link-breaking subprocess of the rewiring process of Gross's model is equivalent to the link-breaking process of the ASIS model. The event that a link is created between a pair of susceptible nodes i and j in a time step happens only if node i or j, but not both, rewires a link to the other with probability R_i/N_i or R_j/N_j, respectively. Hence, by defining ζ and ξ of the ASIS model following the notations in (6), the ASIS model will approximate Gross's model.

For the case that only an initially existing link can be deactivated or activated, Valdez's model [10] applies. By denoting the infection probability by p, the link-deactivation probability by σ, and the curing probability and the link-activation probability by $1/t_R$ and $1/t_B$, respectively, the transform

$$\beta = p, \quad \delta = \frac{1}{t_R}, \quad \zeta = \sigma, \quad \xi = \frac{1}{t_B}, \quad (7)$$

reduces the ASIS model to one with link dynamics similar to Valdez's model [10], ignoring the different disease dynamics in ours and in Valdez's model [10], i.e., the SIS epidemics versus the SIR epidemics.

III. THE STEADY-STATE INFECTION IN THE ADAPTIVE ε-SIS MODEL

Van Mieghem *et al.* [16] showed that the classical SIS model can be exactly formulated in the form of a continuous-time Markov chain with 2^N states. Later, completely independently, Simon *et al.* [17] proposed the same exact SIS equations. Van Mieghem *et al.* [16] also argued that the steady state of the exact SIS model in a finite-size network is the all-healthy state (i.e., the absorbing state of the SIS Markov chain as shown in [16]). Hence, Li *et al.* [18] mentioned (in Secs. I and III A of [18]) that it is impossible to compare the SIS model directly with some mean-field approximations such as the N-intertwined mean-field approximation (NIMFA) proposed by Van Mieghem *et al.* [16,19] or the heterogeneous mean-field (HMF) approximation proposed by Pastor-Satorras and Vespignani [20], because the steady state of these mean-field approximations actually corresponds to the metastable state of the exact SIS model. However, the metastable state is not defined precisely for finite N. Experimentally, one approach for determining the metastable state for finite N is to run many independent simulation instances, compute the average number of infected nodes over time and look for a plateau. The average number of infected nodes at an empirically determined time point of the plateau is defined as the metastable-state value. This is the approach followed by Chakrabarti *et al.* [21]. Unfortunately, this approach requires an assessment of the choice of the time point to calculate the metastable-state value. The assessment depending on the effective infection rate and the topology is usually determined empirically, making the approach inaccurate and less flexible as a simulation method. An alternative way is to define the metastable state by the
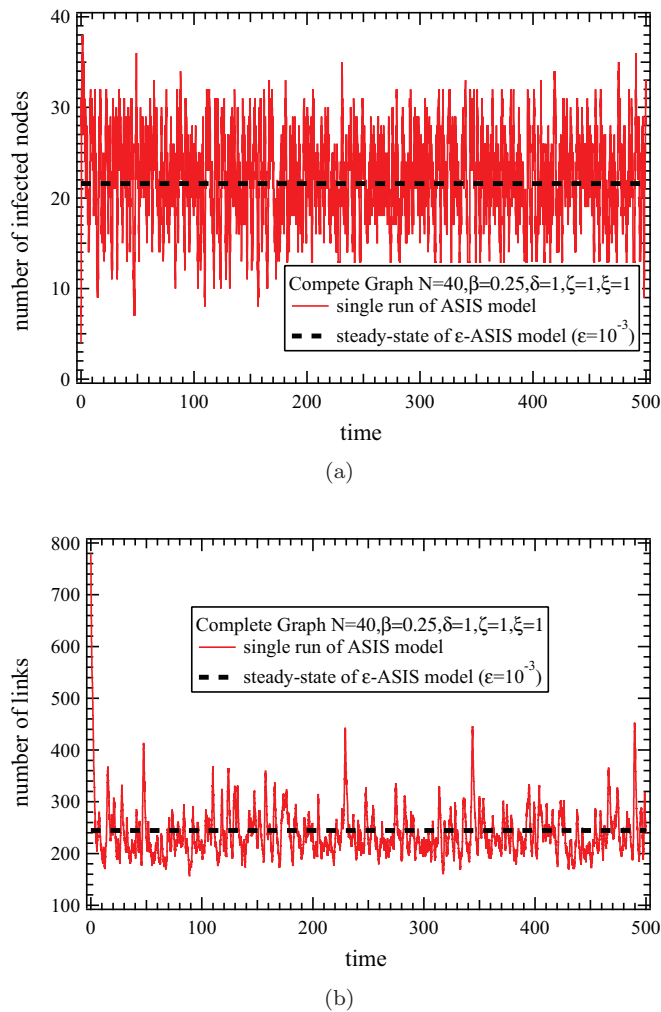
FIG. 2. (Color online) Comparison between the metastable state of the ASIS model (solid red curve) and the steady state of the ε-ASIS model (dashed black straight line). A reasonable instance of a virus outbreak as well as the corresponding link dynamics are shown in (a) and (b), respectively.

steady state of the ε-SIS model [22] for a relatively small ε (e.g., $\varepsilon < \frac{\delta}{N}$). By introducing a nodal self-infection Poisson process in which each node is infected spontaneously with rate ε, the absorbing state of the Markov SIS process is eliminated and thus a nonzero steady state exists for ε > 0. When ε = 0, the ε-SIS model reduces to the classical SIS model.

Li *et al.* [18] employed the ε-SIS model as a benchmark to compare NIMFA [16,19] with HMF [20]. Li *et al.* [18] implemented an event-driven time-continuous simulator of the ε-SIS model (Sec. II A in [18]). Extending the ε-SIS model by introducing the link-dynamic processes (i.e., the link-breaking process and the link-creating process as described in Sec. II A), we name this generalized ε-SIS model incorporating the link dynamics the *adaptive ε-SIS model* (or, *ε-ASIS model*, in short).

Employing the adaptive ε-SIS model with small positive ε, we start a simulation instance in a healthy network and continue to run for a specific warmup period. After the warmup period, the measurement period starts during which we record the change in the value of a metric. Based on the recorded

data, we calculate the average steady-state values of many metrics over the whole measurement period, such as the average number of infected nodes and the average number of links. This calculated time-averaged value is defined as the *average steady-state value* of a metric. We experimentally ensure that the steady state does exist for all simulations and that the initial number of infected nodes in a network has no influence on the steady state. Hence, to calculate the average steady-state value of a metric, we only need to run one simulation instance for a long-enough time period. For any simulation instance, we have taken both the warmup and the simulation period to be 10^4 time units and set the self-infection rate $\varepsilon = 10^{-3}$.

The steady state of the ε-ASIS model will be close to the metastable state of the ASIS model. A reasonable instance of a virus outbreak as well as its corresponding link-dynamic diagram are shown in Figs. 2(a) and 2(b). For instance, the solid curve in Fig. 2(a) denotes a single run of the ASIS model in the metastable state. The dashed line denotes the average steady-state number of infected nodes of the ε-ASIS model. As shown, the steady-state number of infected nodes (dashed black line) of the ε-ASIS model is precisely the line around which the number of infected nodes in the ASIS model fluctuates. These examples illustrate that the steady-state of the ε-ASIS model exists and can be a reasonable approximation to the metastable state of the ASIS model. In this paper, we use the ε-ASIS model to calculate the average metastable value of any metric of the ASIS model.

IV. THE METASTABLE STATE IN A COMPLETE GRAPH K_N

A. The average metastable-state fraction of infected nodes

Denote by $Z = \frac{1}{N} \sum_i X_i$ the fraction of infected nodes and by $y = E[Z^*]$ the average metastable-state fraction of the infected nodes, where Z^* is the fraction of infected nodes in the metastable state. In the same manner, the average value of any other metric in the metastable state can be defined. The governing equations (1) and (2) lead to an expression (11) for the average metastable-state fraction *y* of infected nodes, when the initial topology is a complete graph K_N.

Theorem 1. The average metastable state or maximal fraction $y = E[Z^*]$ of infected nodes in a graph with *N* nodes, produced by (1) and (2) in which $a_{ij}(0) = 1$, satisfies the quadratic equation

$$y^2 - 2Vy + H = 0, \tag{8}$$

where

$$V = 1 - \frac{1}{2N} + \frac{\omega - 1}{2\tau N} \tag{9}$$

and

$$H = 1 - \frac{1}{N} + \mathrm{Var}[Z^*] - E\left[\frac{1}{N^2} \sum_{j=1}^{N} d_j^*(1 - X_j^*)\right]. \tag{10}$$

The solution of (8) is, explicitly,

$$y = \left(1 - \frac{1}{2N} + \frac{\omega-1}{2\tau N}\right)\left\{1 \pm \sqrt{1 - \frac{1 - \frac{1}{N} + \mathrm{Var}[Z^*] - E\left[\frac{1}{N^2}\sum_{j=1}^{N} d_j^*\left(1 - X_j^*\right)\right]}{\left(1 - \frac{1}{2N} + \frac{\omega-1}{2\tau N}\right)^2}}\right\}, \quad (11)$$

where $\mathrm{Var}[Z^*]$ and d_j^* denote the variance of the fraction of infected nodes and the degree of node j, respectively, when $\frac{d}{dt}E[\frac{2L}{\xi} - \frac{(\omega-1)N}{\beta}Z] = 0$ and the corresponding random variables are denoted by $*$.

Proof. See Appendix A. ∎

Although there exist two possible solutions in (11), denoted by y_1 and y_2, only one applies, as proved in Appendix C. If $\tau \to \infty$ with finite ω, the positive sign in (11) is correct; otherwise, the negative sign in (11) applies. When $\omega \to 0$ (i.e., no link dynamics), (8) reduces to the corresponding equation for a fixed complete graph [23].

Given that the initial topology is a complete graph K_N with $N = 40$, we first verify Theorem 1 by simulations for various effective link-breaking rates ω, given a fixed link-creating rate ξ. The exact solution (11) is numerically calculated by substituting the variance $\mathrm{Var}[Z^*]$ and the term $E[\sum_j d_j^* X_j^*]$ obtained from the simulation results into the right part of (11). Then this numerically calculated result is compared with the average metastable-state fraction of infected nodes experimentally obtained. As observed in Fig. 3(a), the exact solution (11) fits the simulation results well for various cases. The term (10) is not larger than 1, which is indeed confirmed by Fig. 3(b).

Furthermore, Fig. 4(a) and Fig. 4(b) illustrate the behavior of y and H versus the effective link-breaking rate ω. Theorem 1 is verified again and the term H is indeed less than 1. As the average metastable-state fraction of infected nodes decreases in the effective link-breaking rate ω, the adaptation of the topology in response to the epidemic spread does suppress the infection.

B. Epidemic threshold

The existence of an epidemic threshold τ_c for a specific finite-size network was reported in the classical SIS model (see, e.g., [16], [24], [25], and [21]). For the effective infection rate $\tau > \tau_c$, a disease can eventually persist and become endemic; otherwise, it will vanish quickly (i.e., the metastable state of the SIS model is the purely healthy state).

Theorem 2. The epidemic threshold in the ASIS epidemic process on K_N equals

$$\tau_c(\omega;\xi) = \frac{\omega - 1}{N\left(h(\omega;\xi) - 2 + \frac{1}{N}\right)}, \quad (12)$$

where $h(\omega;\xi) = \lim_{y\downarrow 0}\frac{H}{y}$ is a positive, slowly varying function obeying, for all $\omega > 0$,

$$1 \leqslant h(\omega;\xi) \leqslant 2 + \frac{1}{N}\left(\frac{1}{\frac{\partial \tau_c(\omega;\xi)}{\partial \omega}\big|_{\omega\to\infty}} - 1\right)$$

and $h(1;\xi) = 2 - \frac{1}{N}$.

Proof. See Appendix B. ∎

Theorem 2 implies that the epidemic threshold τ_c tends to be a linear function of ω since the function $h(\omega;\xi)$ varies slowly in ω, especially for large ω.

Experimentally, we compute the epidemic threshold by setting a baseline y_c on the average metastable-state fraction $y(\tau)$ of infected nodes and by defining τ_c for which $y(\tau_c) = y_c$ as the epidemic threshold for a specific set of parameters $(\delta,\zeta,\xi,\varepsilon)$. Employing this method with $y_c = \frac{1}{N}$, we determine the epidemic threshold τ_c as a function of the effective link-breaking rate ω. The function $h(\omega;\xi)$ can be calculated experimentally by $h = \frac{H(\tau_c)}{y_c}$.
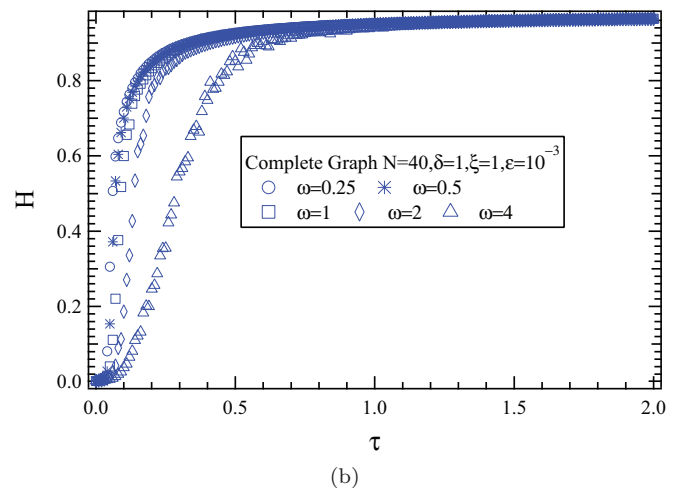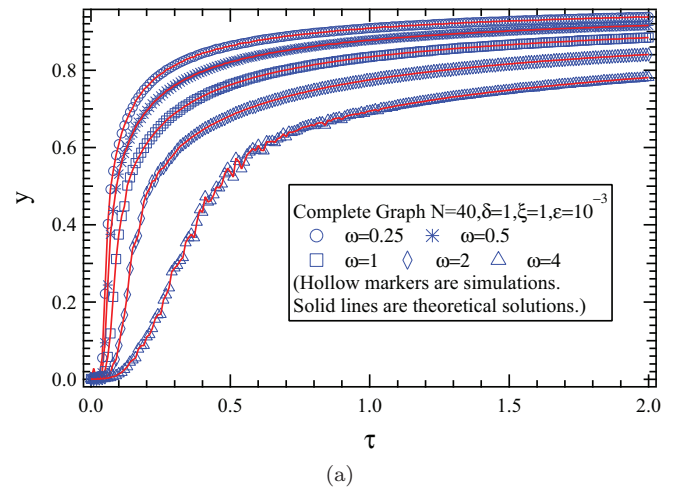

(a)

(b)

FIG. 3. (Color online) (a) Comparison between the formula (11) numerically calculated and the simulation results on the average metastable-state fraction y of infected nodes versus the effective infection rate τ in the network taking complete graph as the initial topology. The blue markers denote the simulation results, while the solid red lines are calculated numerically based on (11). (b) H in (10) corresponding to the cases in (a).
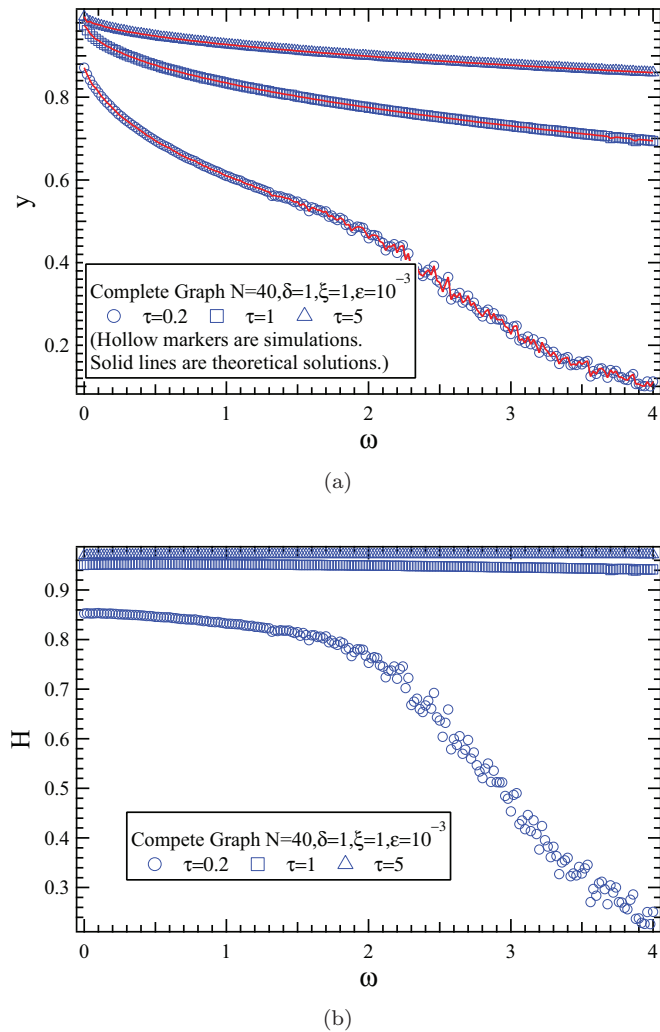
(a)

(b)

FIG. 4. (Color online) (a) Comparison between the formula (11) numerically calculated and the simulation results on the average metastable-state fraction y of infected nodes versus ω when the initial topology is a complete graph, i.e., ASIS model on K_N. The blue markers denote the simulation results while the solid red lines are calculated numerically based on (11). (b) H in (10) corresponding to the cases in (a).

As shown in Fig. 5(b), the function $h(\omega; \xi)$ is indeed a slowly varying function of ω. Specifically, when ω is large, $h(\omega; \xi)$ is almost a constant, as shown in the inset of Fig. 5(b). The epidemic threshold τ_c well approximates a linear function of ω as shown in Fig. 5(a). Both observations are consistent with Theorem 2.

The linear law of the epidemic threshold as a function of the link-breaking rate was also reported by Tunc *et al.* [11] in a similar model based on a mean-field analysis.

C. Metastable-state topology

1. Impact of the disease dynamics on the metastable-state topology

We aim to investigate the impact of the disease dynamics (i.e., the infection process and the curing process) on the metastable-state topology when the initial topology is a complete graph. Some metastable-state topological characteristics such as the connectivity [15], the average number of
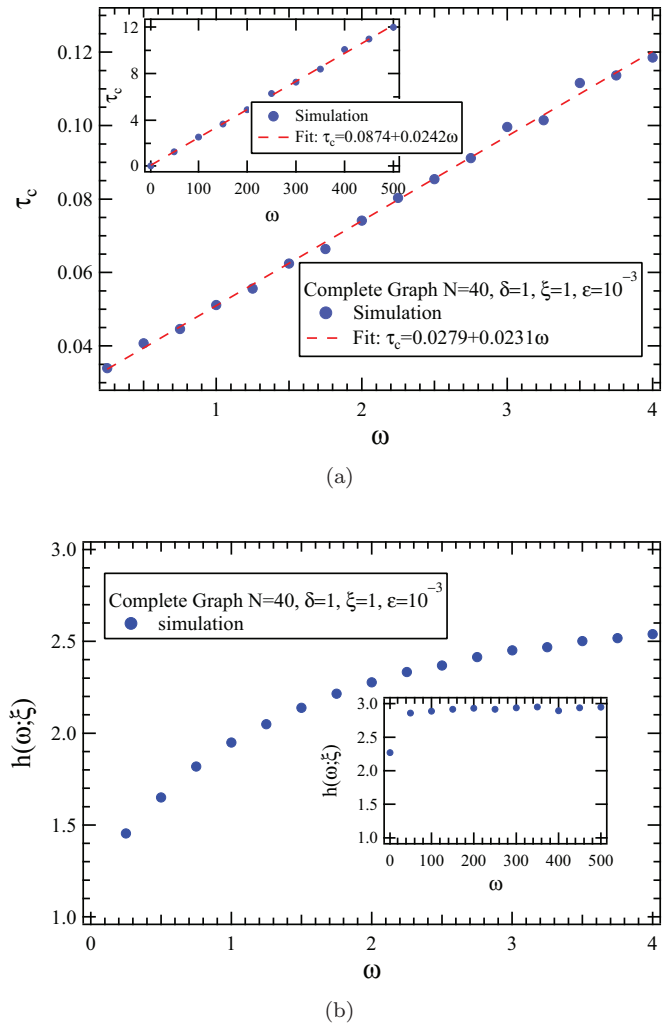

(a)

(b)

FIG. 5. (Color online) (a) Epidemic threshold τ_c versus effective link-breaking rate ω in complete graph of size $N = 40$. The inset shows τ_c for a large range of ω. Simulations (blue circles) are computed by the method described in Sec. IV B. (b) $h(\omega; \xi)$ as a function of ω corresponding to the cases in (a). The inset shows $h(\omega; \xi)$ for a large range of ω.

components, the size of the biggest component [26], the assortativity, the modularity [14], and the number of links are shown. The average metastable-state number of links [normalized by $N(N - 1)$], demonstrated in Fig. 6(a), drops down at the very beginning and then approaches asymptotically a constant as τ increases. The constant plateau goes against the intuition that the number $E[2L^*]/[N(N - 1)]$ of links should be almost 1 if the effective infection rate τ is extremely high because almost all nodes are infected immediately so that no link will be broken. Actually, for a larger range of τ, namely $\tau \in [0, 1500]$, the inset in Fig. 6(a) demonstrates that the number $E[2L^*]/[N(N - 1)]$ of links does rise, albeit rather slowly after the initial dropping. One possible reason for this observation is described as follows. When τ is not high enough, it is very likely that the link between an infectious i and its susceptible neighbor j is broken before i infects j. However, once the link between them was broken, no link between them will be created again, because each node is infected with high
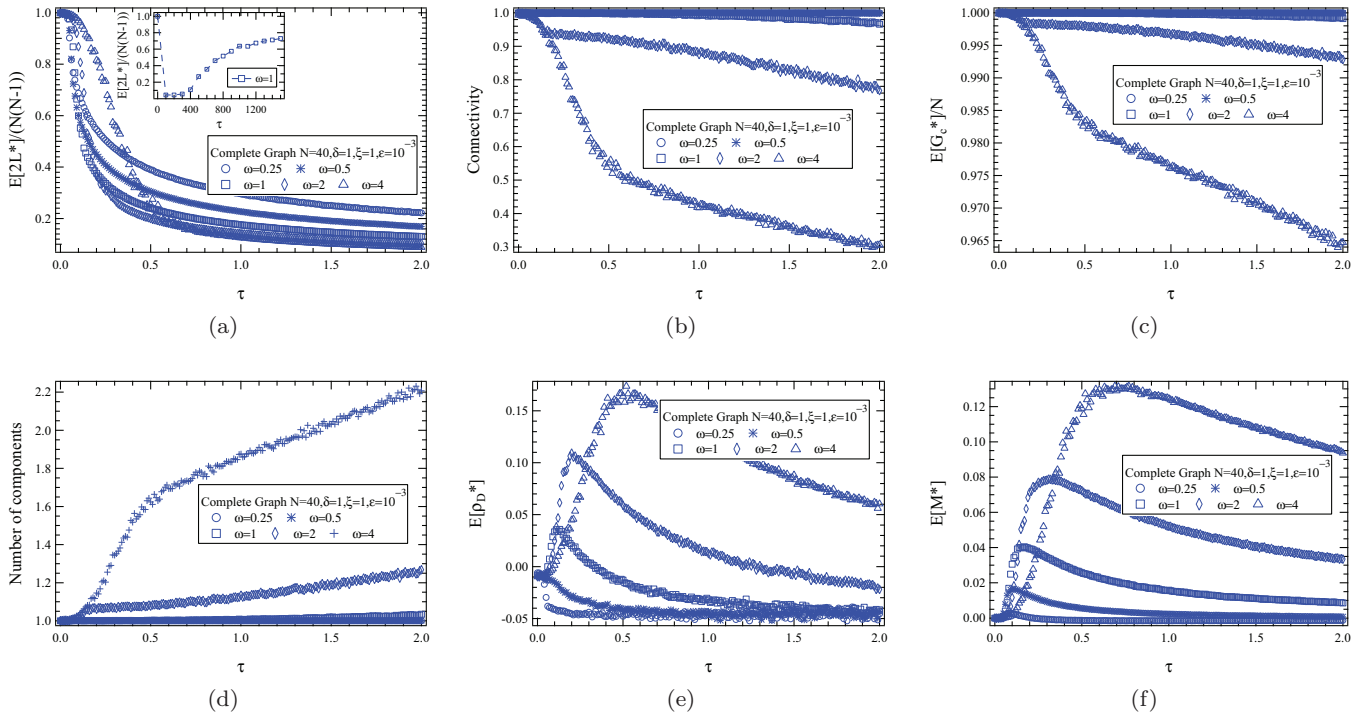
FIG. 6. (Color online) Impact of the effective infection rate τ on the characteristics of the metastable-state topology. (a) The normalized average metastable-state number $\frac{E[2L^*]}{N(N-1)}$ of links versus τ. The inset shows $\frac{E[2L^*]}{N(N-1)}$ for a large range of τ. (b) The metastable-state probability that a graph is connected versus τ. (c) The normalized average metastable-state size $\frac{E[G_c^*]}{N}$ of the biggest component versus τ. (d) The average metastable-state number of components of a graph versus τ. (e) The average metastable-state linear degree correlation coefficient (assortativity) $E[\rho_D^*]$ versus τ. (f) The average metastable-state modularity $E[M^*]$ [14] versus τ.

probability even for a not too high τ and a relatively small ω. The number of links will decrease slowly but gradually. In contrast, the link between i and j tends not to be broken when τ is extremely high (e.g., $\tau \to \infty$) because both nodes are infected with high probability. Other metrics such as the connectivity and the size of the biggest component are correlated to the number of links. Figure 6(b) (the connectivity) illustrates that when the effective link-breaking rate (e.g., $\omega = 2\zeta/\xi > 1$) is relatively high, the network tends to be disconnected. Also, as the effective infection rate τ increases from 0 to a not too high value, the probability of connectivity declines gradually. Figures 6(d) and Fig. 6(c), respectively, show the number of the components and the size of the biggest component of a network in metastable state. The network breaks into a biggest component of size near to N and a few small-size components with high probability for the cases with relatively high $\omega > 1$.

In order to demonstrate the assortativity of the metastable-state topology, the linear degree correlation coefficient ρ_D [27] for an undirected graph is computed as shown in Fig. 6(e). Given that the effective infection rate τ is fixed and the effective link-breaking rate ω is not too large, the larger ω is, the larger is the assortativity of a graph. The introduction of link dynamics with moderate rates promotes the correlation in a network, which was also reported by Gross *et al.* [6]. The modularity [14] behaves the same as the assortativity, as shown in Fig. 6(f). The observation that a high modularity leads to a high assortativity indicates that the modularity is correlated to the assortativity [28].

The high modularity also indicates an apparent division on the topology. Thus, we claim that after introducing a link-breaking process, the structure of a network is divided into two loosely interconnected components consisting of susceptible nodes and infected nodes, called the S component and the I component, respectively. The link-creating process enhances the intraconnectivity in the S component, while the link-breaking process degrades the interconnectivity between the S component and the I component. On the other hand, both the infection process and the curing process ruin the division between the S component and the I component. Figure 6(e) shows that as the disease dynamics and the link dynamics compete, the assortativity reaches its maximum followed by a drop down as the effective infection rate increases. So does the modularity shown in Fig. 6(f). The division between S and I components also appears in other adaptive models such as the one proposed by Gross *et al.* [6].

2. Impact of the link dynamics on the metastable-state topology

In this section, we focus on the impact of the link dynamics (including the link-breaking process and the link-creating process) on the metastable-state infection and topology. In other words, for a fixed effective infection rate τ, we investigate some metrics in metastable state as a function of the effective link-breaking rate ω. For a fixed τ, the average metastable-state fraction y of infected nodes decreases as ω increases, which is demonstrated in Fig. 4(a). This also implies that the epidemic threshold τ_c grows up as ω increases. Since the epidemic
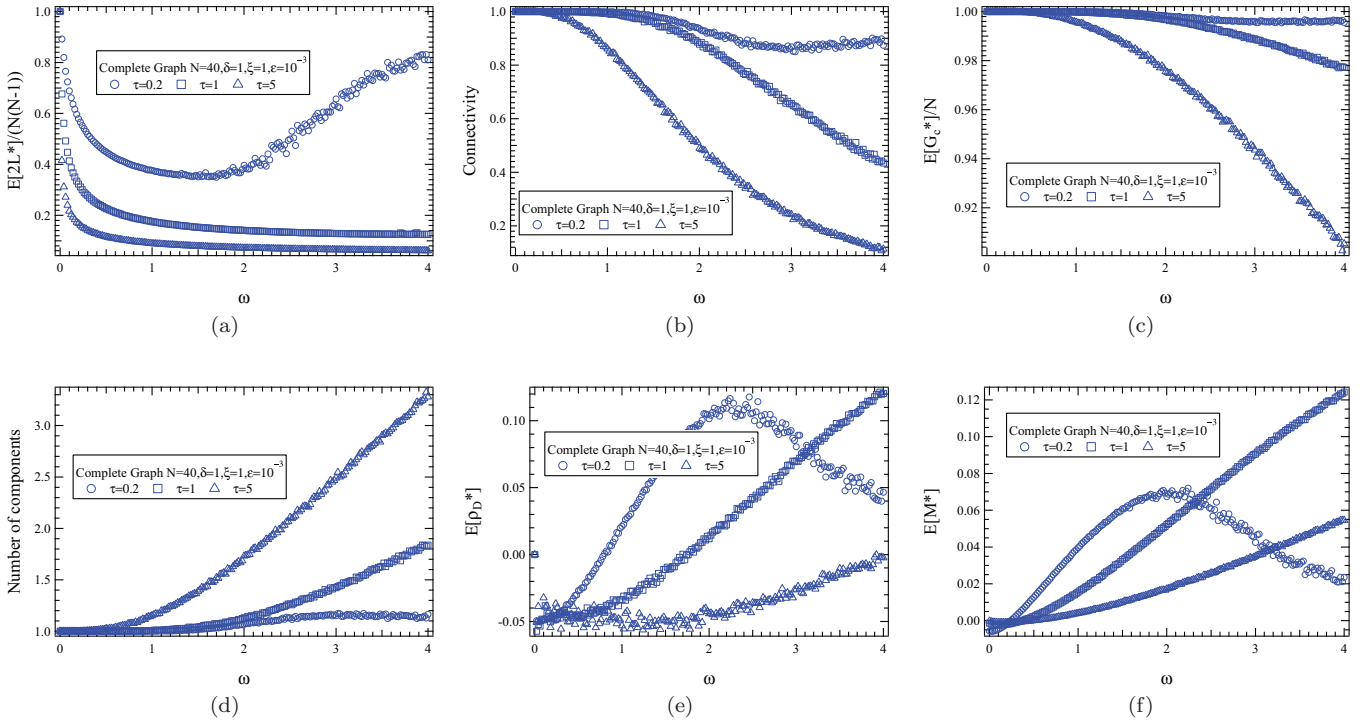
FIG. 7. (Color online) Impact of the effective link-breaking rate ω on the characteristics of the metastable-state topology such as (a) the normalized average metastable-state number $\frac{E[2L^*]}{N(N-1)}$ of links, (b) the probability that a graph is connected in the metastable state, (c) the normalized average metastable-state size $\frac{E[G_c^*]}{N}$ of the biggest component, (d) the average number of components of a graph in the metastable state, (e) the average metastable-state linear degree correlation coefficient (assortativity) $E[\rho_D^*]$, and (f) the average metastable-state modularity $E[M^*]$ [14].

threshold $\tau_c > 1/(N-1)$ [16] for a complete graph of size N is the smallest among all graphs of size N and that a network will become a noncomplete graph after introducing link-dynamic processes, the epidemic threshold τ_c will always be larger than $1/(N-1)$ given that $\omega \geqslant 0$.

The network becomes more sparse as the effective link-breaking rate ω increases, as shown in Fig. 7(a). However, for the case ($\tau = 0.2$) there is a drop followed by an uncommon rise in the number of the links. This observation is explained in Appendix D based on the analysis of the existence state of each link. For the connectivity, Fig. 7(b) shows that a network will be disconnected with high probability if $\omega > 1$ under the condition ($\delta = 1, \xi = 1$). Figures 7(c) and 7(d) show that the size of the biggest component behaves the same as the connectivity and that the higher τ is, the

more disconnected components the network will break into. Moreover, the assortativity $E[\rho_D^*]$ of the network will increase and then decline as ω increases, as shown in Fig. 7(e). The introduction of the link dynamics will increase the assortativity of a network, which was also reported by Gross *et al*. [6]. As shown in Fig. 7(f), the modularity behaves in a way similar to that of the assortativity.

3. Structure of the metastable-state topology

In Secs. IV C1 and IV C2, the metastable-state topological properties are demonstrated for some special combinations of parameters. This section provides an overview on the metastable-state topology in terms of the modularity, connectivity, and degree distribution.
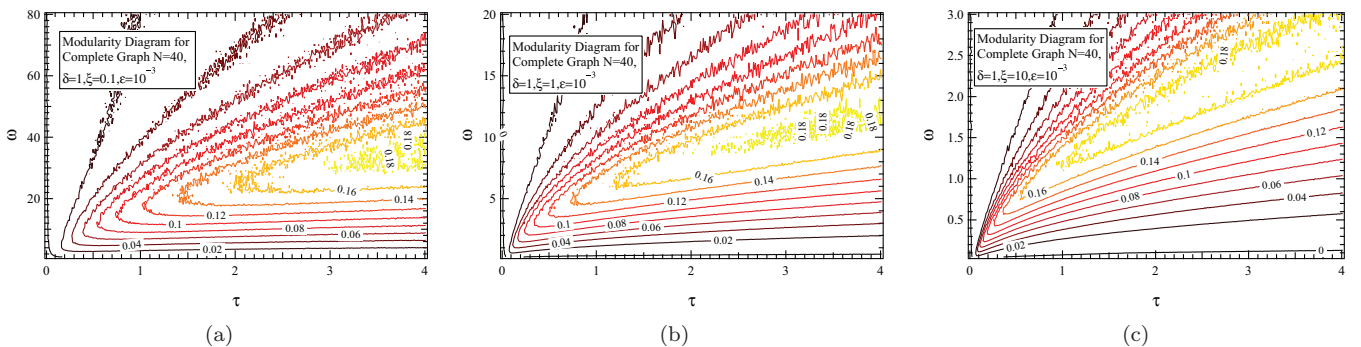

FIG. 8. (Color online) Modularity contours in the $\tau - \omega$ plane for three different values of link-creating rate ξ, namely, (a) $\xi = 0.1$, (b) $\xi = 1$, and (c) $\xi = 10$.
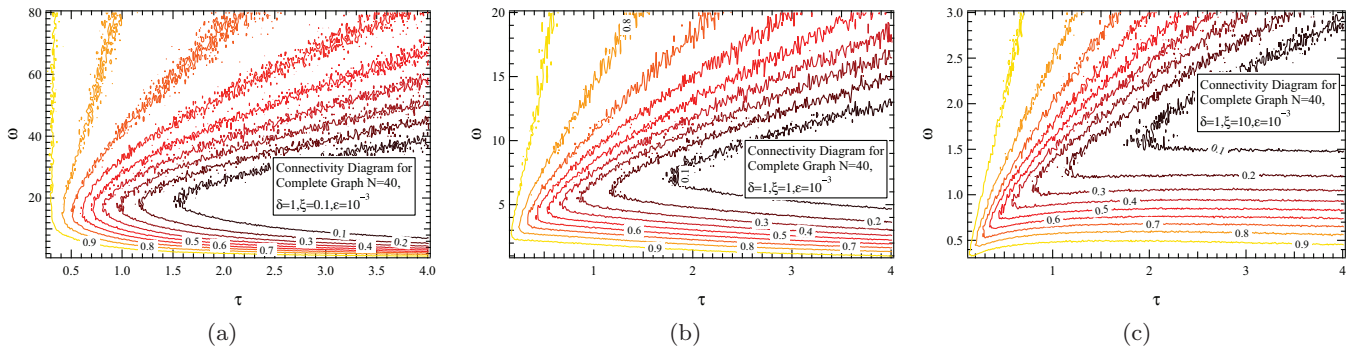
FIG. 9. (Color online) Connectivity contours in the $\tau - \omega$ plane for three different values of link-creating rate ξ, namely, (a) $\xi = 0.1$, (b) $\xi = 1$, and (c) $\xi = 10$.

Figures 8(b) and Fig. 9(b) demonstrate, respectively, the modularity diagram and the connectivity diagram in a τ, ω plane with $\delta = 1, \xi = 1$. The metastable-state topology of the ASIS model shows high modularity within a "half-open elliptical-like" domain where τ is relatively high, ω is not too high, and $\tau \ll \omega$. This can be explained as follows. According to its definition [14], the high modularity means (i) that the infected nodes and the susceptible nodes are well separated and (ii) that the I component is comparable in size to the S component. For the domains with low τ, the number of infected nodes is extremely low. Because the network is partitioned based on the viral states of nodes in order to compute its modularity (explained in [14]), a low fraction of infected nodes (i.e., the size of the I component is small) will induce a low modularity. For the domains with extremely high ω, the infection will be strongly suppressed, which also leads to a low modularity. Moreover, the connectivity shown in Fig. 9(b) behaves in contrast to the modularity in the τ, ω plane. The high connectivity is achieved at the expense of a low modularity as the network is compact and a noticeable separation of the susceptible and the infectious communities (components) does not emerge. Naturally, for extremely low values of τ the network is likely to be connected with high probability, independent on the link-breaking rate ω. For a fixed relatively high value of τ, high connectivity could be achieved either for (a) extremely high ω, which corresponds to the high adaptability of the network that suppresses the virus spread and prevents the high connectivity of the S component being ruined, or (b) extremely low ω, which corresponds to the weak link dynamics that is not fast enough to separate the infected nodes from the susceptible nodes. In what follows, we take as examples the regions of high ω [i.e., the above case (a)] in Figs. 9(a)–9(c) to explain some interesting observations. High connectivity can be achieved for high ω as demonstrated. The higher the link-creating rate ξ is, the higher the link-breaking rate ζ has to be to keep the topology connected, although the ratio ω of ζ to ξ decreases. To illustrate this, let us consider the curves for the connectivity equal to 0.7 in Figs. 9(a)–9(c). Fixed $\tau = 1$ corresponds to $\omega \approx 40, 12, 2$, as shown. Meanwhile, the corresponding $\zeta = 2, 6, 10$ because $\omega = 2\zeta/\xi$, which increases as ξ increases from 0.1 to 10. The higher ξ is, the denser the S component consisting of all susceptible nodes becomes. For a given τ and a high ξ, if ζ is not high enough to separate the I component from the S

component and once one of the susceptible node is infected, many other nodes in the S component will be infected soon. Consequently, the number of S-I links increases and thus more link-breaking events tend to happen, which ruins the connectivity. Thus, ζ should become higher as ξ increases in order to keep a specific connectivity. The increase in ζ is not linearly proportional to the increase in ξ in order to keep a specific connectivity and thus $\omega = 2\zeta/\xi$ decreases. Moreover, the "concentric half-open elliptical-like" connectivity regions always exist, albeit slightly different from each other. Hence, it is anticipated that the half-open concentric elliptical-like contour line is a universal diagram of the connectivity as well as the modularity in a τ, ω plane for any link-creating rate ξ.

Besides the modularity and the connectivity, the metastable-state degree distribution is another important characteristic to investigate. Unfortunately, it is hard to provide an overview of the degree distribution due to its complexity. Instead, we just investigate some extreme cases, namely, $\tau \ll \{\zeta, \xi\}$ and $\tau \gg \{\zeta, \xi\}$, while ensuring $\tau > \tau_c$, as shown in Fig. 10. For other cases, the distributions are hard to depict. Figure 10(a) demonstrates the degree distributions for susceptible and infected nodes for these extreme cases. As shown in Fig. 10(a), the degree distribution for susceptible nodes is a binomial-like one with a peak near $N - 1$ for the case with $\tau \ll \{\zeta, \xi\}$, while it is a binomial-like one with a medium mean value for $\tau \gg \{\zeta, \xi\}$. In other words, the impact of link dynamics, if much stronger than the disease dynamics (i.e., $\tau \ll \{\zeta, \xi\}$), may induce a high-mean-value degree distribution for susceptible nodes. The degree distribution for infected nodes centers at a low value for the case with high τ or at a high value for the case with low τ. Based on the above observations, the degree distribution for all nodes is depicted as follows [also shown in Fig. 10(b)]. For $\tau \ll \{\zeta, \xi\}$, the degree distribution centers nearly $N - 1$ with low variance, owning one peak [e.g., the case with ($\tau = 0.007, \zeta = \xi = 0.07$)] or multiple peaks [e.g., the case with ($\tau = 0.08, \zeta = \xi = 10$)] but only one is noticeable. In contrast, for $\tau \gg \{\zeta, \xi\}$, the degree distribution is a binomial-like distribution with low mean value for high τ [e.g., the case with ($\tau = 0.08, \zeta = \xi = 0.001$)] or high mean value for low τ [e.g., the case with ($\tau = 0.0065, \zeta = \xi = 0.0005$)]. In the following, we explain how the binomial-like degree distribution could emerge for cases with $\tau \gg \{\zeta, \xi\}$. Because the S component (consisting of all susceptible nodes) is well mixed with the I component
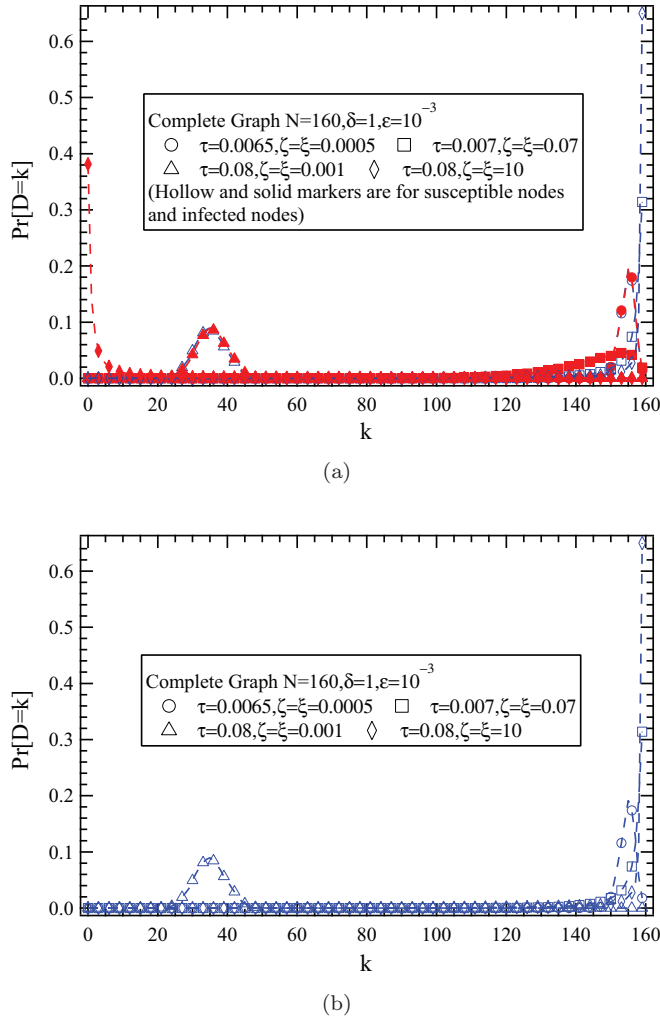
(a)

(b)

FIG. 10. (Color online) The metastable-state degree distributions for (a) susceptible and infected nodes, and (b) for all nodes.

(consisting of all infected nodes) for the case with $\tau \gg \{\zeta,\xi\}$, the link-breaking event happens between any nodal pair with almost the same probability, which could be considered as a random link-removing. Randomly removing links from a regular graph (e.g., a complete graph) will induce a topology with the binomial degree distribution

$$\Pr[D = k] = \binom{N-1}{k} p_L^k (1 - p_L)^{(N-1-k)}, \qquad (13)$$

where N and p_L denote the size of the network and the link density after deletion. Hence, if substituting the normalized metastable-state number of links to the right part of (13), we will obtain a metastable-state degree distribution similar to the distribution experimentally obtained.

D. Determination of the bistability in the ASIS model

In this section, we concentrate on the distribution $\Pr[Z^*]$ of the metastable-state fraction Z^* of infected nodes rather than the average metastable-state fraction $y = E[Z^*]$ of infected nodes. Figure 11 demonstrates the distribution of Z^* for cases with various effective infection rate τ and fixed link-dynamic rates ζ and ξ. For low ($\tau = 0.15$), the metastable state is
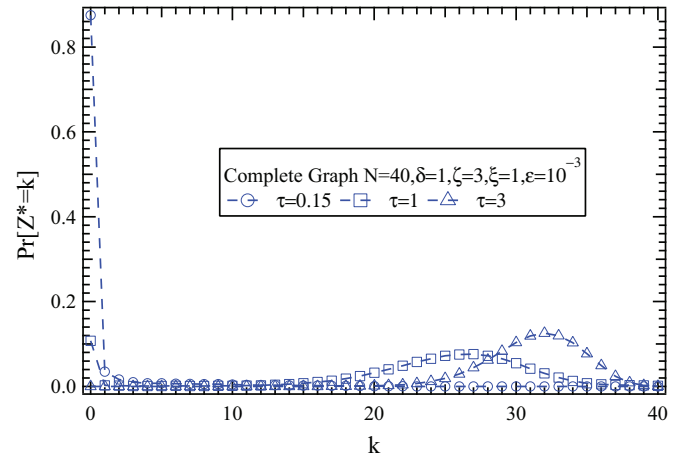

FIG. 11. (Color online) The distribution of the metastable-state fraction Z^* of infected nodes.

close to the healthy state, while the metastable state is the endemic state for the case with high ($\tau = 3$). However, the metastable-state fraction Z^* of infected nodes is around either 0 or a nonzero positive value for some other case (e.g., the case $\tau = 1$ shown in Fig. 11). For the case $\tau = 1$, the probability that the metastable state is the healthy state (i.e., $\Pr[Z^* = 0]$) is comparable in value to the probability that the metastable state is the endemic state (i.e., $\Pr[Z^* = c]$), where c is a positive value depending on τ. This indicates that maybe the metastable state is stable in either of two dramatically different infection states, which is likely the bistability phenomenon. The bistability phenomenon in adaptive networks in the presence of disease dynamics was first reported by Gross *et al.* [6]. The bistable state is a metastable state where there is no infection in the ASIS model or the infection persists in the ASIS model on average.

If the probability $\Pr[Z^* = 0]$ is comparable in value with the probability $\Pr[Z^* = c]$ for a specific τ, where the factor c depends on τ, we plot these two values simultaneously
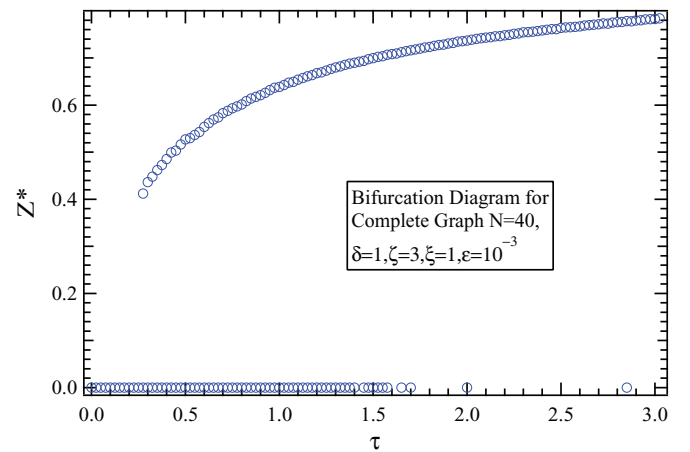

FIG. 12. (Color online) The bifurcation diagram of the metastable-state fraction of infected nodes. The metastable-state infection of the ASIS model is in the healthy state (for $0 \leqslant \tau \leqslant 0.3$), the bistable infection state (for $0.3 \leqslant \tau \leqslant 1.6$), and the endemic state (for $\tau \geqslant 1.6$), in sequence, as the effective infection rate τ increases.

in a τ, Z^* plane and think that the metastable state of the ASIS model is possibly stable in either of the two states. Otherwise, if one probability is extremely higher than the other in value, or there exists only one peak in $\Pr[Z^*]$ versus τ, we consider that the metastable state is stable just in one infection state. Following the above-mentioned manner, we plot Fig. 12 showing a bifurcationlike behavior in the ASIS model. It seems that the metastable state changes from the healthy state, to the bistable state, and to the endemic state as τ increases. Because of the similarity between the ASIS model and Gross's model [6] discussed previously in Sec. II C, we argue that the bistability phenomenon may also exist in the ASIS model when concentrating on Z^* rather than its average value.

V. CONCLUSION

In order to characterize the coevolution and interplay between the dynamics on a network (i.e., disease dynamics) and the dynamics of the network (i.e., dynamics of the link state), we proposed an adaptive network model named $ASIS$, where a link-breaking Poisson process with rate ζ and a link-creating Poisson process with rate ξ are introduced in the classical SIS model. For the case that the initial topology of an adaptive network is a complete graph, we deduced the average metastable-state fraction of infected nodes (see Theorem 1). Furthermore, we derived a linear law of the epidemic threshold τ_c versus the effective link-breaking rate $\omega = 2\zeta/\xi$ (see Theorem 2). The phase transition that a disease can persist in the presence of link dynamics for the effective infection rate $\tau > \tau_c$ and the linear function $\tau_c(\omega)$ are also experimentally verified.

Simulations reveal how the disease dynamics and the link dynamics promote an adaptive network evolving into a topology with specific characteristics in terms of the number of links, the connectivity, the size of the biggest component, the modularity, and the assortativity. Nodes in the network are divided into two loosely interconnected components according to their viral states, namely the I (infectious) component and the S (susceptible) component, based on which the modularity [14] is calculated. When the disease dynamics dominate (i.e., the infection process is faster than the link-breaking process and the link-creating process in rate), the network evolves to one with a binomial-like degree distribution, no apparent community structure, and disassortative mixing. When the link dynamics are much faster than the disease dynamics in rate, the degree distribution is composed of multiple peaks and the topology becomes a little, but clearly, modular and assortative. For the other cases than those described above, it is hard to sketch the topology. Nevertheless, a universal contour-line behavior is observed from the modularity diagram in the τ, ω plane. Either a very low effective infection rate τ or a very high effective link-breaking rate ω will lead to the region of low modularity and disassortative mixing. The connectivity is opposite to the modularity, meaning that a low connectivity leads to a high modularity in the ASIS model.

Finally, rather than the average metastable-state fraction of infected nodes, the investigation on the distribution of the infection fraction reveals that between the healthy state and the endemic state there may exist a bistable state where the metastable-state infection fraction is stable either around 0

(i.e., the healthy state) or around a positive nonzero value (i.e., the endemic state).

APPENDIX A: PROOF OF THEOREM 1

We transform the link dynamic Eq. (2) into

$$
\begin{aligned}
\frac{d}{dt}E[a_{ij}] = {} & \xi(1 - E[a_{ij}]) - \xi E[(X_i + X_j)] \\
& - (\zeta - \xi)E[a_{ij}(X_i + X_j)] + \xi E[X_i X_j] \\
& + (2\zeta - \xi)E[a_{ij}X_i X_j].
\end{aligned}
$$

After summing these equations over all $j \neq i$ and using the degree of node i, $d_i = \sum_{j=1}^{N} a_{ij}$ and $a_{ii} = 0$, we obtain

$$
\begin{aligned}
& \frac{d}{dt}E[d_i] \\
&= \xi(N - 1 - E[d_i]) - \xi E\left[(N-1)X_i + \sum_{j=1;j\neq i}^{N} X_j\right] \\
&\quad - (\zeta - \xi)E\left[d_i X_i + \sum_{j=1}^{N} a_{ij}X_j\right] \\
&\quad + \xi E\left[X_i \sum_{j=1;j\neq i}^{N} X_j\right] + (2\zeta - \xi)E\left[\sum_{j=1}^{N} a_{ij}X_i X_j\right].
\end{aligned}
$$

Using

$$
(N-1)X_i + \sum_{j=1;j\neq i}^{N} X_j = (N-2)X_i + \sum_{j=1}^{N} X_j
$$

and

$$
X_i \sum_{j=1;j\neq i}^{N} X_j = X_i\left(\sum_{j=1}^{N} X_j - X_i\right) = X_i \sum_{j=1}^{N} X_j - X_i,
$$

we find

$$
\begin{aligned}
\frac{d}{dt}E[d_i] = {} & \xi(N - 1 - E[d_i]) - \xi E\left[(N-1)X_i + \sum_{j=1}^{N} X_j\right] \\
& - (\zeta - \xi)E\left[d_i X_i + \sum_{j=1}^{N} a_{ij}X_j\right] \\
& + \xi E\left[X_i \sum_{j=1}^{N} X_j\right] + (2\zeta - \xi)E\left[\sum_{j=1}^{N} a_{ij}X_i X_j\right].
\end{aligned}
$$

Substituting

$$E\left[\sum_{j=1}^{N} a_{ij} X_i X_j\right] = -\frac{1}{\beta}\frac{d}{dt}E[X_i] - \frac{1}{\tau}E[X_i]$$
$$+ E\left[\sum_{j=1}^{N} a_{ij} X_j\right]$$

from (1) into the above relation to remove the highest order correlation term yields

$$\frac{d}{dt}E[d_i]$$
$$= \xi(N-1) - \xi E[d_i] - \xi E\left[\left(N-1+\frac{(2\zeta-\xi)}{\tau\xi}\right)X_i\right]$$
$$- \xi E\left[\sum_{j=1}^{N} X_j\right] - (\zeta-\xi)E[d_i X_i] + \xi E\left[X_i \sum_{j=1}^{N} X_j\right]$$
$$- \frac{(2\zeta-\xi)}{\beta}\frac{d}{dt}E[X_i] + \zeta E\left[\sum_{j=1}^{N} a_{ij} X_j\right].$$

Rewritten, using $\omega = \frac{2\zeta}{\xi}$,

$$\frac{d}{dt}E\left[\frac{d_i}{\xi} + \frac{(\omega-1)}{\beta}X_i\right]$$
$$= N-1-E\left\{d_i + \left[N-1+\frac{\omega-1}{\tau} + \left(\frac{\omega}{2}-1\right)d_i\right]X_i\right\}$$
$$- E\left[\sum_{j=1}^{N} X_j\right] + E\left[X_i \sum_{j=1}^{N} X_j\right] + \frac{\omega}{2}E\left[\sum_{j=1}^{N} a_{ij} X_j\right].$$

Now we sum over all i, using $\sum_{i=1}^{N} d_i = 2L$; then

$$\frac{d}{dt}E\left[\frac{2L}{\xi} + \frac{(\omega-1)}{\beta}\sum_{i=1}^{N} X_i\right]$$
$$= N(N-1) - E\left[2L + \left(N-1+\frac{\omega-1}{\tau}\right)\sum_{i=1}^{N} X_i\right]$$
$$+ \left(\frac{\omega}{2}-1\right)\sum_{i=1}^{N} d_i X_i\right] - E\left[N\sum_{j=1}^{N} X_j\right]$$
$$+ E\left[\left(\sum_{i=1}^{N} X_i\right)^2\right] + \frac{\omega}{2}E\left[\sum_{j=1}^{N} d_j X_j\right].$$

Simplified, with $\tilde{t} = \delta t$ and the fraction of infected nodes $Z = \frac{1}{N}\sum_{j=1}^{N} X_j$,

$$\frac{d}{d\tilde{t}}E\left[\frac{2\delta L}{\xi} + \frac{(\omega-1)N}{\tau}Z\right]$$
$$= N(N-1) - N\left(2N-1+\frac{\omega-1}{\tau}\right)E[Z]$$
$$+ N^2 E[Z^2] + E\left[\sum_{i=1}^{N} d_i X_i\right] - E[2L].$$

When the derivative at the left-hand side vanishes (in the steady-state or at an extreme value, which we denote by a superscript ∗), we have

$$N(N-1) - N\left(2N-1+\frac{\omega-1}{\tau}\right)E[Z^*] + N^2 E[Z^{*2}]$$
$$- E\left[\sum_{i=1}^{N} d_i^* \left(1-X_i^*\right)\right] = 0.$$

Using $E[Z^2] = \text{Var}[Z] + (E[Z])^2$ and $y = E[Z^*]$, we arrive at (8). Solving the quadratic equation (8) finally yields (11). ∎

APPENDIX B: PROOF OF THEOREM 2

From the quadratic equation (8), we find for $y > 0$ that

$$V = \frac{1}{2}\left(y + \frac{H}{y}\right).$$

Using the definition (9) of V, we can extract τ as

$$\tau = \frac{\omega-1}{2N\left[\frac{1}{2}\left(y+\frac{H}{y}\right)-1+\frac{1}{2N}\right]}.$$

The epidemic threshold is defined as the largest non-negative value of τ when $y \downarrow 0$, such that

$$\tau_c = \frac{\omega-1}{N\left(\lim_{y\downarrow 0}\frac{H}{y}-2+\frac{1}{N}\right)},$$

where $\frac{H}{y} = q(\tau,\omega;\xi)$ is a function of both τ and ω (and ξ) [29], but $\lim_{y\downarrow 0}\frac{H}{y} = q(\tau_c,\omega;\xi) = h(\omega;\xi)$. Thus, we obtain the analytic expression (12) for epidemic threshold. The remainder of the proof consists of demonstrating that $h(\omega;\xi)$ is a positive, slowly varying function.

The two roots of (8) satisfy $y_1 + y_2 = 2V$ and $y_1 y_2 = H$. Since $H \geqslant 0$, the roots are either both negative or both positive. Since negative roots have no physical meaning, we must require that $V \geqslant 0$, which implies, with the definition (9) that

$$\frac{1-\omega}{2N\left(1-\frac{1}{2N}\right)} \leqslant \tau.$$

This condition for the effective infection rate τ, which is only confining for $\omega < 1$, can be sharpened. The roots y_1 and y_2 must be real so that the discriminant of (8) is non-negative, $H \leqslant V^2$ or $(\sqrt{H}-V)(\sqrt{H}+V) \leqslant 0$. Requiring positive roots so that $0 \leqslant \sqrt{H} \leqslant V$, leads, with the definition (9) of V, to

$$\frac{\omega-1}{2N\left(\sqrt{H}+\frac{1}{2N}-1\right)} \geqslant \tau.$$

Since $\sqrt{H}+\frac{1}{2N}-1 < 0$, we arrive at the improved lower bound

$$\frac{1-\omega}{2N\left(1-\frac{1}{2N}-\sqrt{H}\right)} = \tau^* \leqslant \tau. \qquad \text{(B1)}$$

If $\omega \geqslant 1$ (more link breaking than link creation), then there is no confinement for τ.

Since (B1) indicates, for $\omega < 1$, that $\tau^* \leqslant \tau_c$, there must hold for $\omega < 1$ that $2\sqrt{H} \leqslant h(\omega;\xi) < 2 - \frac{1}{N}$. In particular,

$h(0;\xi) \geqslant 1$ because $\tau_c(0;\xi) \geqslant \frac{1}{N-1}$, the epidemic threshold in SIS epidemics in K_N without link dynamics. More precisely [23], with $\tau_c(0;\xi) = \frac{1}{N}[1 + \frac{c}{\sqrt{N}} + O(N^{-1})]$, we find

$$h(0;\xi) = 1 + \frac{c}{\sqrt{N}} + O(N^{-1}).$$

A continuity argument requires for $\omega \to 1$ that $\tau_c > 0$ so that $\lim_{\omega \to 1} h(\omega;\xi) = 2 - \frac{1}{N}$ and $\tau_c(1;\xi) = \frac{1}{N \frac{\partial h(\omega;\xi)}{\partial \omega}|_{\omega=1}}$. For $\omega > 1$ to have an epidemic threshold $\tau_c(\omega;\xi) > 0$, it must be that $h(\omega;\xi) > 2 - \frac{1}{N}$. For an extremely high effective link-breaking rate ω, an infected node is immediately isolated from the healthy nodes almost surely and cures in isolation so that the epidemic threshold $\tau_c(\omega;\xi)$ is increasing for all $\omega > 1$ and that $\lim_{\omega \to \infty} \tau_c(\omega;\xi) = \infty$. It is reasonable to assume that $h(\omega;\xi)$ is not decreasing in ω for any $\omega \geqslant 0$, in which case we deduce from (12) that $\lim_{\omega \to \infty} \frac{\partial h(\omega;\xi)}{\partial \omega} = 0$ and that $h(\omega;\xi) \leqslant 2 + \frac{1}{N}(\frac{1}{\frac{\partial \tau_c(\omega;\xi)}{\partial \omega}|_{\omega \to \infty}} - 1)$ for all $\omega > 1$. ∎

APPENDIX C: SIGN BEFORE THE SQUARE ROOT IN (11)

The roots of the quadratic equation (8) satisfy $y_1 y_2 = H$ and $0 \leqslant y_1 y_2 \leqslant 2 - \frac{1}{N}$. If $H \geqslant 1$, then not both can be smaller than 1. Since $V \geqslant 1$ in this case (due to $H \leqslant V^2$), (11) shows that the physically relevant root ($0 \leqslant y_1 \leqslant 1$) is obtained with the minus sign. When $H \leqslant 1$, both y_1 and y_2 can lie in the $[0,1]$ interval and the hyperbola $y_1 y_2 = H$ shows that

$$y_1 \leqslant \sqrt{H} \leqslant y_2.$$

If $H \leqslant 1 \leqslant V$, implying that $\omega \geqslant 1 + \tau$, then again the negative sign in (11) applies.

If $H \leqslant V^2 \leqslant V \leqslant 1$, implying that $\omega \leqslant 1 + \tau$, then the situation becomes more complex and both signs in (11) seem to be possible. In the limit case where $H \ll V$, (11) shows that $y_2 \simeq 2V$ so that again the negative sign applies if $V > \frac{1}{2}$ and $H \ll V$. Finally, we show that a positive sign can occur. If $\tau \to \infty$ (and ω finite), in which case $X_j^* \to 1$ and $\text{Var}[Z^*] = 0$, then (8) reduces to

$$y^2 - \left(2 - \frac{1}{N}\right)y + 1 - \frac{1}{N} = 0,$$

from which

$$y = \left(1 - \frac{1}{2N}\right) \pm \sqrt{\left(1 - \frac{1}{2N}\right)^2 - \left(1 - \frac{1}{N}\right)}$$
$$= \left(1 - \frac{1}{2N}\right) \pm \frac{1}{2N}.$$

Since $y = 1$, the plus sign is required.

APPENDIX D: THE METASTABLE LINK PROBABILITY p_{ij}

In the metastable state (where $\frac{dE[a_{ij}(t)]}{dt} = 0$), we deduce from (2) that

$$\zeta E[a_{ij}(X_i - X_j)^2] = \xi E[(1 - a_{ij})(1 - X_i)(1 - X_j)]. \quad \text{(D1)}$$

By the Cauchy-Schwarz inequality, we have

$$E[a_{ij}(X_i - X_j)^2] \leqslant \sqrt{E[a_{ij}^2]E[(X_i - X_j)^4]}$$
$$= \sqrt{E[a_{ij}]E[(X_i - X_j)^2]}.$$

Using the metastable link probability $p_{ij} = E[a_{ij}] = \Pr[a_{ij} = 1]$, the following inequality arises:

$$\xi^2\{E[(1 - a_{ij})(1 - X_i)(1 - X_j)]\}^2 \leqslant p_{ij}\zeta^2 E[(X_i - X_j)^2]. \quad \text{(D2)}$$

Similarly for the other term,

$$E[(1 - a_{ij})(1 - X_i)(1 - X_j)]$$
$$\leqslant \sqrt{E[(1 - a_{ij})^2]E[(1 - X_i)^2(1 - X_j)^2]}$$
$$= \sqrt{E[(1 - a_{ij})]E[(1 - X_i)(1 - X_j)]},$$

we find the inequality

$$\zeta^2\{E[a_{ij}(X_i - X_j)^2]\}^2 \leqslant (1 - p_{ij})\xi^2 E[(1 - X_i)(1 - X_j)], \quad \text{(D3)}$$

which, after reworking, leads to

$$\xi^2 E[(1 - X_i)(1 - X_j)] - \zeta^2\{E[a_{ij}(X_i - X_j)^2]\}^2$$
$$\geqslant p_{ij}\xi^2 E[(1 - X_i)(1 - X_j)].$$

Combining both bounds yields, with $\omega = \frac{2\zeta}{\xi}$ and (D1),

$$\frac{\{E[a_{ij}(X_i - X_j)^2]\}^2}{E[(X_i - X_j)^2]} \leqslant p_{ij} \leqslant 1 - \frac{\omega^2}{4}\frac{\{E[a_{ij}(X_i - X_j)^2]\}^2}{E[(1 - X_i)(1 - X_j)]}.$$

Approximating $\leqslant$ by $\approx$ in the bounds (D2) and (D3) leads, after introducing into the metastable link condition (D1), to

$$\zeta^2 p_{ij} E[(X_i - X_j)^2] \approx \xi^2(1 - p_{ij})E[(1 - X_i)(1 - X_j)].$$

We estimate that the metastable link probability $p_{ij} = E[a_{ij}] = \Pr[a_{ij} = 1]$ is about

$$p_{ij} \approx \frac{\xi^2 E[(1 - X_i)(1 - X_j)]}{\zeta^2 E[(X_i - X_j)^2] + \xi^2 E[(1 - X_i)(1 - X_j)]}$$
$$= \frac{1}{1 + \omega^2 \frac{E[(X_i - X_j)^2]}{4E[(1 - X_i)(1 - X_j)]}}. \quad \text{(D4)}$$

The derivation for the link density (D4) is physically meaningful, despite the approximations. Equation (D4) qualitatively corresponds with the simulations of the normalized average metastable-state number $E[2L^*]/[N(N - 1)]$ of links (i.e., the link density) shown in Fig. 7(a). In the following, we take as an example the case $\tau = 0.2$ (the blue circles) in Fig. 7(a).

For ω close to zero (the "weakly adaptive" region), the metastable-state topology is almost the initial topology K_N and we have a high link density (close to 1). Further, for $\omega \in [0,1.5]$, we have a quadratic decrease in ω. Then the link density p_{ij} reaches its minimum near $\omega = 1.5$, as the term $\frac{E[(X_i - X_j)^2]}{4E[(1 - X_i)(1 - X_j)]}$ in (D4) decreases in the same order of magnitude as ω^2. Finally, for $\omega \in [1.5,\infty]$, the link dynamics strongly suppresses the infection on the network, $X_i \approx X_j \approx 0$,

so that the term $\frac{E[(X_i - X_j)^2]}{4E[(1-X_i)(1-X_j)]} \to 0$ and decreases faster than ω increases; hence, the influence of ω vanishes and the link density is again 1.

For a fixed τ, the connectivity behaves in a similar way as the link density p_{ij} does. Figure 9(b) shows that even

the regions with dramatically different effective link-breaking rates, e.g., the "weakly adaptive" region with very low ω and the "strongly adaptive" region with very high ω, can have the same connectivity. As ω increases, the connectivity decreases, reaches its minimum, and increases to 1.

[1] I. B. Schwartz and L. B. Shaw, Physics **3**, 17 (2010).

[2] S. Funk, S. Salathé, and V. A. A. Jansen, J. R. Soc. Interface **7**, 1247 (2010).

[3] T. Gross and B. Blasius, J. R. Soc. Interface **5**, 259 (2008).

[4] E. Volz and L. A. Meyers, J. R. Soc. Interface **6**, 233 (2009).

[5] B. A. Prakash, H. Tong, N. Valler, M. Faloutsos, and C. Faloutsos, in *Machine Learning and Knowledge Discovery in Databases*, Lecture Notes in Computer Science, edited by J. L. Balcázar, F. Bonchi, A. Gionis, and M. Sebag, Vol. 6323 (Springer, Berlin, Heidelberg, 2010), pp. 99–114.

[6] T. Gross, Carlos J. Dommar D'Lima, and B. Blasius, Phys. Rev. Lett. **96**, 208701 (2006).

[7] V. Marceau, P.-A. Noël, L. Hébert-Dufresne, A. Allard, and L. J. Dubé, Phys. Rev. E **82**, 036116 (2010).

[8] D. H. Zanette and S. Risau-Gusmán, J. Biol. Phys. **34**, 135 (2008).

[9] C. Lagorio, M. Dickison, F. Vazquez, L. A. Braunstein, P. A. Macri, M. V. Migueles, S. Havlin, and H. E. Stanley, Phys. Rev. E **83**, 026102 (2011).

[10] L. D. Valdez, P. A. Macri, and L. A. Braunstein, Phys. Rev. E **85**, 036108 (2012).

[11] I. Tunc, M. Shkarayev, and L. Shaw, J. Stat. Phys. **151**, 355 (2013).

[12] S. Wieland, T. Aquino, and A. Nunes, Europhys. Lett. **97**, 18003 (2012).

[13] T. Rogers, W. Clifford-Brown, C. Mills, and T. Galla, J. Stat. Mech.: Theory Exp. (2012) P08018.

[14] Calculating the modularity M involves explicitly a special division of nodes into interconnected subcomponents (subgroups). Based on this division, we calculate the modularity M by Eq. (2) proposed by P. Van Mieghem, X. Ge, P. Schumm, S. Trajanovski, and H. Wang [Phys. Rev. E **82**, 056113 (2010)]. In this paper, the modularity appears as a measurement of clusterness between the component S consisting of all susceptible nodes and the component I consisting of all infected nodes. If M is high, it means that the components S and I are well separated.

[15] The connectivity in this paper is defined as the probability that the graph is connected. In other words, it is the probability that the biggest connected component contains all N nodes in the graph.

[16] P. Van Mieghem, J. Omic, and R. Kooij, IEEE/ACM Trans. Networking **17**, 1 (2009).

[17] P. L. Simon, M. Taylor, and I. Kiss, J. Math. Biol. **62**, 479 (2011).

[18] C. Li, R. van de Bovenkamp, and P. Van Mieghem, Phys. Rev. E **86**, 026116 (2012).

[19] E. Cator and P. Van Mieghem, Phys. Rev. E **85**, 056111 (2012).

[20] R. Pastor-Satorras and A. Vespignani, Phys. Rev. E **63**, 066117 (2001).

[21] D. Chakrabarti, Y. Wang, C. Wang, J. Leskovec, and C. Faloutsos, ACM Trans. Inf. Syst. Secur. **10**, 1 (2008).

[22] P. Van Mieghem and E. Cator, Phys. Rev. E **86**, 016116 (2012).

[23] E. Cator and P. Van Mieghem, Phys. Rev. E **87**, 012811 (2013).

[24] R. Pastor-Satorras and A. Vespignani, Phys. Rev. E **65**, 035108 (2002).

[25] A. Ganesh, L. Massoulie, and D. Towsley, in *Proceedings of 24th Annual Joint Conference of the IEEE Computer and Communications Societies INFOCOM 2005, Miami, FL, 13–17 March 2005*, edited by K. Makki and E. Knightly, Vol. 2 (IEEE, New York, 2005), pp. 1455–1466.

[26] The biggest component refers to the connected component with the largest number of nodes. For large N, the biggest component becomes the giant component.

[27] P. Van Mieghem, H. Wang, X. Ge, S. Tang, and F. A. Kuipers, Eur. Phys. J. B **76**, 643 (2010).

[28] P. Van Mieghem, X. Ge, P. Schumm, S. Trajanovski, and H. Wang, Phys. Rev. E **82**, 056113 (2010).

[29] Besides the two ratios τ and ω, we need the link-creation rate ξ (or β or ζ) to determine the time relation that couples the link dynamics to the epidemic process.